ELSEVIER

Materials Science and Engineering B101 (2003) 266–269

MATERIALS SCIENCE & ENGINEERING B

www.elsevier.com/locate/mseb

Non-constant anodization current effects on spectra of porous silicon LEDs

G. Barillaro [a,*], A. Diligenti [a], M. Piotto [b], M. Allegrini [c], F. Fuso [c], L. Pardi [c]

[a] *Dipartimento di Ingegneria dell'Informazione, Università di Pisa, Via Diotisalvi 2, Pisa 56126, Italy*

[b] *Centro di Studio per Metodi e Dispositivi per Radiotrasmissioni, Via Diotisalvi 2, Pisa 56126, Italy*

[c] *INFM, Dipartimento di Fisica "Enrico Fermi", Università di Pisa, Via Buonarroti 2, Pisa 56127, Italy*

Received 6 November 2002; accepted 23 November 2002

Abstract

Porous silicon (PoSi) LEDs are today under investigation for integration of optoelectronic silicon devices with standard microelectronic circuits. The electrical and optical properties of these devices depend on the anodization parameters (current density and time) of the PoSi formation process. However, a constant anodization current is generally used to fabricate the active PoSi layer of LEDs, and only few works exist in which a non-constant anodization current is reported. In this work, a study of the anodization current effects on the electroluminescence (EL) spectra of PoSi LEDs having around 0.1% of external quantum efficiency is presented. Several anodization current waveforms (constant, linear, triangular, and trapezoidal) were used to fabricate layers with different mechanical and optical properties. EL spectra of fabricated devices are reported and discussed.

Keywords: Porous silicon; Light-emitting diode; Electroluminescence spectra

1. Introduction

Silicon-based optoelectronic devices represent today an active field of research due to the possibility of on-chip integration with standard microelectronic circuits. Porous silicon (PoSi) and other light-emitting silicon-based materials contain nanostructures or crystallites in the nanometer range, that modify the optical properties of crystalline silicon by quantum confinement of electrons and holes in the small volume of nanocrystals. As a matter of fact, PoSi layers can efficiently emit light in the visible part of electromagnetic spectrum at room temperature when excited with photons (photoluminescence) or electrons (electroluminescence (EL)).

PoSi light-emitting diodes (LEDs) are probably the most attractive application of PoSi (for a review, see [1]), although several other optical devices, like detectors, wave guides, and switches are under investigation [2,3]. In less than 10 years, significant progress has been achieved: LEDs emitting throughout the visible spectrum have been fabricated and the best measured external quantum efficiency (EQE) at room temperature has risen from 10^{-5}% for early Schottky-like devices [4] to 0.1% for the next generation p–n junction devices [5]. Electrical and optical characteristics of these devices basically depend on the fabrication process as well as the properties (morphological, electrical, and optical) of PoSi, which in turn depend on the anodization process parameters (current density, HF concentration, temperature, etc.). Although the fabrication processes of LEDs can be quite different, the PoSi layer is generally produced by means of anodization in HF solution using a constant current density with a proper value in order to obtain a higher porosity and then a better EQE.

In this work, several different anodization current waveforms (constant, linear, triangular, and trapezoidal) were used to fabricate PoSi layers with different optical properties in an LED structure fully compatible with an industrial process. The effects of constant and non-constant current anodization on the EL spectra of LEDs are presented and discussed.

* Corresponding author. Tel.: +39-050-568657; fax: +39-050-568522.

E-mail address: g.barillaro@ing.unipi.it (G. Barillaro).

0921-5107/03/$ - see front matter © 2003 Elsevier Science B.V. All rights reserved.
doi:10.1016/S0921-5107(02)00694-3

2. Fabrication process

The fabrication process of the LED structure is detailed in Ref. [6] and only briefly reported here. It is based on an industrial BCD (bipolar+CMOS+DMOS) process and schematically consists of the following steps: (1) wet oxidation (90 nm) of a p-type ⟨1 0 0⟩ wafer with a doping of 10^{15} cm^{-3}; (2) boron implantation through the oxide to create a grid-like pattern, 1.4 μm deep, with a higher p-doping (pBody)—grid lines are 4 μm wide and several hundreds microns long; (3) arsenic implantation to define an n^+ contact 0.23 μm deep on the pBody lines; (4) polysilicon deposition (450 nm) and polysilicon n^+ implantation; (5) polysilicon patterning to define the front contact (constituted by a poly/SiO_2 structure) and the lines to the active (luminescent) area; (6) deposition of an LPCVD Si_3N_4 layer with a thickness of 90 nm; this film acts as a masking layer during the anodization process, as will be clear later; (7) deposition of a spinnable SiO_2 (TEOS) layer (500 nm) to be used as a mask for the Si_3N_4 etching; (8) definition of a window onto the SiO_2 to expose the active area; (9) wet Si_3N_4 etching by means of a H_3PO_4 solution; and (10) etch of the residual oxide. An Al metal contact was evaporated on the back of sample and annealed at 400 °C in nitrogen. The final step was the selective anodization of the structure through the Si_3N_4 window. The anodization process, performed in the dark, acts only on p-doped silicon, whereas the n^+ poly/n^+ layers are not affected. In this way a p-PoSi layer is formed and the n^+ poly/n^+ silicon contact is left unchanged, so that the fabrication of an electrical contact on PoSi after its formation is unnecessary. The composition of the solution was 1:1 (by volume) HF (48%):C_2H_5OH (99.9%). After the anodization, the samples were rinsed in acetone and cyclohexane and freeze-dried in order to avoid cracks in the PoSi structure. The LED structure is sketched in Fig. 1.

Since the PoSi formation occurs along anodization current paths, if the doping of the p-silicon is uniform under the n^+ contact a crystalline pillar is not affected by the polarization process [7]. A current leakage crystalline path then exists between the contact and the substrate when the LED is biased. In our structure, the presence of a graded p-doping forces the anodization current under the n^+ contact, so leading to a continuous buried PoSi layer under the contact. When the border of the anodized (porous) volume reaches the highly doped p-region, the current lines bend under the contact, and the anodization proceeds at a higher rate in that area (Fig. 1b). In this way, under bias conditions, the injected current completely flows through the PoSi active layer and no leakage crystalline path exists, so yielding a better EQE; EQE of the order of 0.1% or greater has been achieved for our devices [8].

3. Results and discussion

A constant current density with a proper high value (of the order of 50 mA cm^{-2} or greater) is generally used for anodization of PoSi LEDs in order to produce a PoSi layer with good optical properties. In fact, high current densities give rise to PoSi layers with higher porosity and better optical properties than those produced by low current density, though with worse mechanical properties (more brittle material). Furthermore, a negative gradient of porosity exists when silicon substrate is anodized with a constant current [9], resulting in a large distribution of nanocrystals size and then in wide EL spectra. Again, when the anodization current is constant an abrupt profile exists at the high-porosity PoSi layer–crystalline interface that could affect the electrical properties of LEDs. In fact, it is well known that for compound semiconductor heterostructures an abrupt bandgap change between two materials reduces the injection current efficiency with respect to a smooth transition [10].

We fabricated LEDs using both constant and non-constant anodization current densities, as detailed in Table 1. A constant value of 75 mA cm^{-2} in the first case and a top value of 90 mA cm^{-2} in the other cases were used to produce a PoSi active layer with high porosity and then high internal quantum efficiency. In fact, we found that PoSi layers produced by means of non-constant anodization have better mechanical prop-

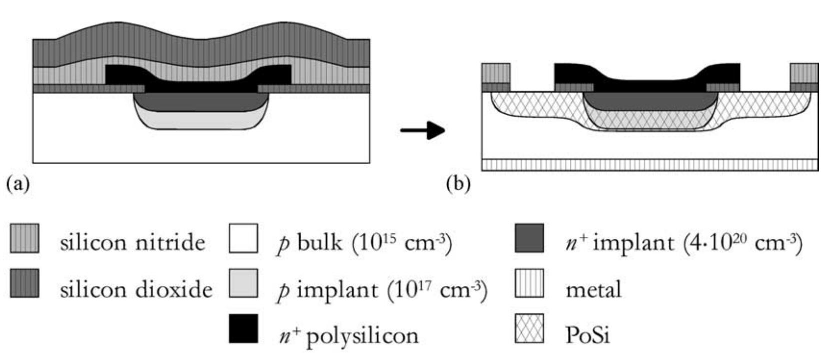

Fig. 1. Schematic process fabrication of LEDs.

Table 1

Anodization current density		Anodization time duration (s)
Waveform	Value	
Constant	75 mA cm^{-2} for 60 s	60
Linear	25–90 mA cm^{-2} for 65 s	65
Triangular	25–90 mA cm^{-2} for 65 s 90–25 mA cm^{-2} for 5 s	70
Trapezoidal	25–90 mA cm^{-2} for 10 s 90 mA cm^{-2} for 25 s 90–25 mA cm^{-2} for 10 s	45

erties, so that it is possible to employ higher current density for PoSi formation, without that apparent macroscopic cracks occur during the drying process. This could be explained with the lower average porosity of PoSi layer. Non-constant anodization currents having linear, triangular, and trapezoidal waveforms were investigated to improve mechanical and optical characteristics of PoSi layers. Depending on the anodization current setting, the anodization time was properly chosen to achieve a continuous PoSi layer between the polycontact and the substrate, so avoiding current leakage through a crystalline pillar.

Yellow-orange EL is clearly visible for LEDs by the naked eye in room lighting with forward polarization (injection current and voltage around 10 mA and 10 V, respectively) for devices with an active area of 800 μm × 800 μm. The polarity of voltage bias is defined such that it is positive when the back Al contact is positive with respect to the front polycontact. An HP4145B parameter analyzer was used for electrical measurements of the samples. A typical $I-V$ curve of a device (anodization parameters: linear current density from 25 to 90 mA cm^{-2}, time 65 s) is shown in Fig. 2. It can be noted that a high series resistance (about 700 Ω), limiting the forward current conduction, exists. The presence of high series resistance in LEDs can be ascribed to (i) the resistance of the polycontact lines and the crystalline substrate (about 350 Ω), existing in the device before the anodization process, and (ii) the resistance of the PoSi layer which depends on the anodization conditions. The presence of this series resistance accounts for the relatively high threshold voltage at which EL occurs.

EL spectra are shown in Fig. 3 for different current waveforms. They were acquired by a 320 mm monochromator (Jobin Yvon TRIAX), equipped with a 1200 g mm^{-1} grating and a back-illuminated CCD detector, cooled by LN_2 (Jobin Yvon IOTA ONE). Slit width of 0.5 mm and integration time of 0.5 s were typically used, which, thanks to the high efficiency of the devices, ensured acquisition of spectra with a good signal-to-noise ratio. All spectra were acquired in similar injection

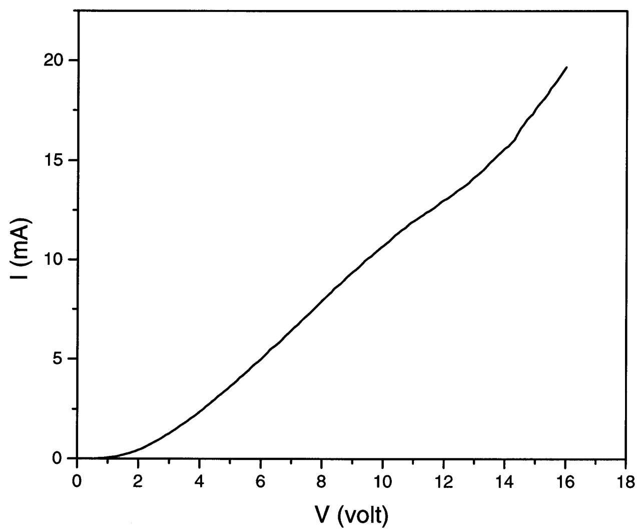

Fig. 2. Typical current–voltage characteristic of LEDs.

current conditions, typically set around 10% above the threshold current. Intensity of all spectra displayed in the figure was normalized to a common value. In any case, EQE of all samples was in the same order of magnitude as that of the device analyzed in Ref. [8], i.e. around 0.1%.

It is clear from Fig. 3 that some important differences occur in EL spectra for samples anodized with non-constant current waveforms with respect to those anodized with a constant current. For instance, LED fabricated with constant current density (75 mA cm^{-2}) shows an EL spectrum peaked at a lower wavelength (700 nm), whereas spectra obtained from devices produced by means of non-constant current density are generally peaked above 800 nm. This fact can be explained with the higher average porosity of LEDs produced with a constant current; in fact, the time-averaged current density of samples anodized with non-constant waveforms is lower, so yielding a PoSi layer with a lower porosity. Moreover, it is interesting to note that samples fabricated with linear, triangular, and trapezoidal waveforms show narrower spectra. Since it is known that spectral width is a function of the nanocrystal size distribution, our findings suggest that a more homogeneous distribution is achieved in non-constant waveform conditions. In other words, a linear increase of the anodization current density might compensate the porosity gradient produced by a constant current density.

Thus, the first result of our investigation is that spectral features of EL are markedly modified when non-constant anodization waveforms are used. More subtle differences exist depending on the choice of the waveform. In particular, emission towards the infrared tail of the spectrum is stronger in the sample produced

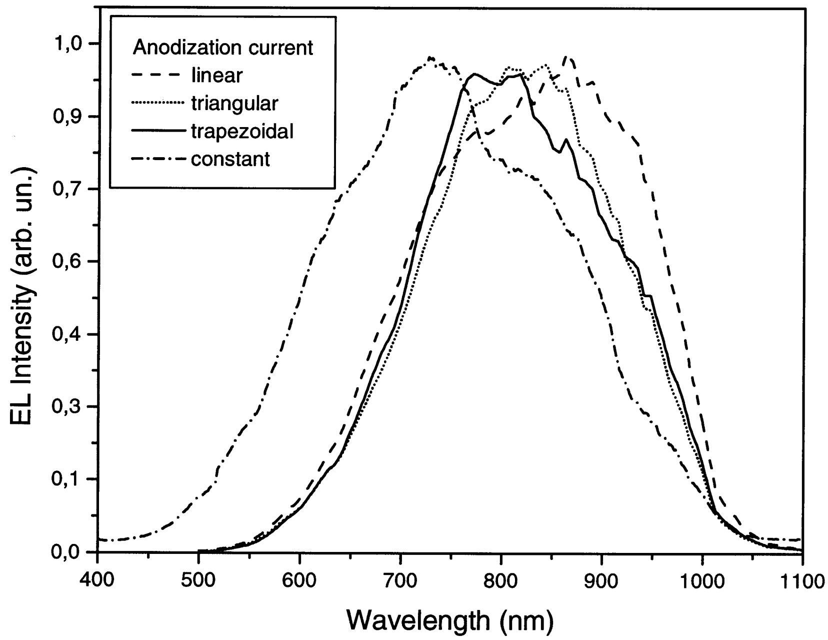

Fig. 3. EL spectra of LEDs for different current waveforms. All spectra were acquired in similar injection current conditions. Intensity of all spectra displayed in the figure was normalized to a common value. EQE of all samples was about 0.1%.

with a linear waveform. Moreover, EL peak seems to shift toward higher energy when the waveform is changed from linear to triangular and then trapezoidal. Based on the comparison with the device anodized at constant current, we infer that triangular or trapezoidal waveforms lead to a larger average porosity of the PoSi layer with respect to the linear one.

4. Conclusions

PoSi LEDs, fully integrated with a standard industrial process, were fabricated with EQE around 0.1%. Analysis of EL emitted by LEDs produced in different anodization conditions confirms the expected sensitivity of the spectral features on the microstructure of the PoSi layer. Indications have been found which can be used to produce samples with an efficient emission peaked in different portions of the spectrum by simply acting on the anodization process, i.e. the last step of the whole fabrication procedure.

Further work will be performed to include the role of local electron transport and charge injection in our interpretation of the experimental results. To this aim, space-resolved EL analysis is planned, which is expected to shed light on the effective space distribution of electron-stimulated light-emitting centers.

Acknowledgements

Work supported by CNR through Progetto Finalizzato MADESS II.

References

[1] P.M. Fauchet, J. Lumin. 80 (1999) 53.
[2] L.A. Balagurov, D.G. Yarkin, G.A. Petrovicheva, E.A. Petrova, A.F. Orlov, S.Ya. Andryushin, J. Appl. Phys. 82 (9) (1997) 4647.
[3] M. Takahashi, N. Koshida, J. Appl. Phys. 86 (9) (1999) 5274.
[4] N. Koshida, H. Koyama, Appl. Phys. Lett. 60 (1992) 347.
[5] A. Loni, A.J. Simons, T.I. Cox, P.D.J. Calcott, L.T. Canham, Electron. Lett. 31 (1995) 1288.
[6] G. Barillaro, F. Pieri, U. Mastromatteo, Opt. Mater. 17 (1–2) (2001) 95.
[7] K.K. Higa, T. Asano, Jpn. J. Appl. Phys. 35 (1996) 6648.
[8] G. Barillaro, A. Diligenti, F. Pieri, F. Fuso, M. Allegrini, Appl. Phys. Lett. 78 (26) (2001) 4154.
[9] M. Thonissen, S. Billat, M. Kruger, H. Luth, G. Berger, U. Frotscher, U. Rossow, J. Appl. Phys. 80 (5) (1996) 2990.
[10] K.D. Choquette, Proc. IEEE 85 (11) (1997) 1730.